Available online at www.sciencedirect.com
ScienceDirect
Coordination Chemistry Reviews 252 (2008) 1052–1068
COORDINATION CHEMISTRY REVIEWS
www.elsevier.com/locate/ccr

Review

Coordination properties of polyamine-macrocycles containing terpyridine units

Carla Bazzicalupi, Andrea Bencini, Antonio Bianchi *, Andrea Danesi, Enrico Faggi, Claudia Giorgi, Samuele Santarelli, Barbara Valtancoli

Department of Chemistry, University of Florence, Via della Lastruccia 3, 50019 Sesto Fiorentino, Italy

Received 31 May 2007; accepted 31 July 2007
Available online 6 August 2007

Dedicated to the memory of the late Prof. Fernando Pulidori.

Contents

Abstract

The insertion of 2,2′:6′,2″-terpyridine groups into macrocyclic polyamine structures gives rise to a considerable enhancement of molecular rigidity which affects their coordination properties. This review concerns some examples of both very rigid, shape-persistent Schiff-base macrocycles and less rigid polyamine-macrocycles in which the rigidity of terpyridine is associated with the flexibility of aliphatic polyamine chains. Structural, thermodynamic, electrochemical, and spectroscopic properties of transition metal complexes with these ligands are presented and correlated with the ligand structures. The ability of some complexes to bind and activate substrate molecules, in particular CO_2 uptake and conversion into carbonate/carbamate, and ATPase mimicking, is also described. The review includes an introductive overview of the relevant terpyridine properties.

Keywords: Terpyridine; Macrocycles; Polyamines; Metal complexes; Substrate activation

1. Introduction

2,2′:6′,2″-Terpyridine (terpyridine, tpy) was isolated for the first time in the early 1930s by Morgan and Burstall [1] from the reaction products obtained by heating at 340 °C 8 kg of pyridine and 1.5 kg of $FeCl_3$ in an autoclave at 50 atm for 36 h. Fifty-five grams of terpyridine was isolated from the mixture containing bipyridine, as a principal compound, along with a huge number of other nitrogen derivatives. Subsequently, terpyridine remained a rare tridentate ligand, mostly employed for coordination studies [2,3] and colorimetric metal determination [4,5], until in the 1990s it was recognized as a pivotal component for the construction of molecular devices [6,7] and supramolecular assemblies [8]. From this point on, interest in terpyridine increased continuously, thanks to the design and the synthesis of a variety of sophisticated derivatives tailored for a wide range of applications. Indeed, terpyridine units have been incorporated into supramolecular dendrimers [8–20] and polymers [21–29], they have been used for surface functionalization [30–37], for the assembly of molecular machines performing controlled linear [38–40] and rotatory [41–44] movements, for the preparation of wire-type components [45–56], helicates [57–59], nanotubes [60], molecular cycles [61–72], wheels [73] and scorpionates [74], for the synthesis of polyamine macrocyclic receptors showing unusual activity in CO_2 fixation [75,76] and ATPase mimicking [77], for the preparation of compounds

* Corresponding author.
E-mail address: antonio.bianchi@unifi.it (A. Bianchi).

0010-8545/$ – see front matter © 2007 Elsevier B.V. All rights reserved.
doi:10.1016/j.ccr.2007.07.024

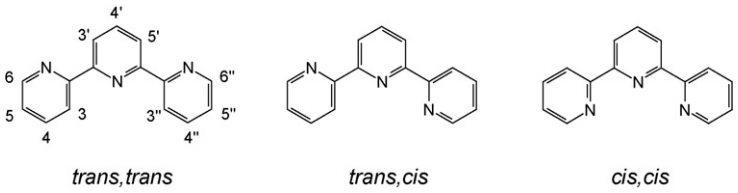

Fig. 1. The three possible conformations of terpyridine.

with antitumoral activity [78–81], for applications in nuclear medicine [82,83] and magnetic resonance imaging [84,85], in addition to many other uses [86].

Nonetheless, the modern chemistry of terpyridine [87] is still founded on its coordination of transition metal ions. Indeed, coordination of two terpyridine units to such metal ions can afford a firm connecting unit for the assembly of extended structures and, in contrast with bidentate ligands (L–L), such as bipyridine, which form chiral $[M(L–L)_3]$ complexes, the $\{M(L–L–L)_2\}$ motif formed by terpyridine and its symmetrically substituted derivatives is achiral. The last characteristic is particularly important when $\{M(tpy)_2\}$ units are used for the assembly of multinuclear systems, since a unique species is formed instead of a mixture of different isomers. Furthermore, as already shown by early work [6], metal complexes with new terpyridine-based ligands display special redox and photophysical properties according to the behaviour of the parent unsubstituted precursors. An additional property, which has promoted the interest in terpyridine, is the size of its complexes. The dimensions of the $\{M(tpy)_2\}$ motif, measured as the distance between the furthest atoms of the two terpyridine units, both across a single ligand and across the metal centre, exceed 1 nm, and thus all systems based upon the $\{M(tpy)_2\}$ motif fall within the domain of nano-sciences.

When terpyridine is incorporated into macrocyclic structures, the resulting ligand molecules acquire conformational rigidity. Such rigidity may lead to shape-persistent macrocycles characterized by fortified cavities which can be exploited for different applications [88].

In the present review we collect information on the coordination properties of terpyridine-based polyamine-macrocycles characterized by different degrees of molecular rigidity, and highlight the special chemical and physico-chemical characteristics, including substrate activation properties, shown by the relevant metal complexes. Shape-persistent polyamine-macrocycles have been generated by the formation of cyclic Schiff-base derivatives, displaying preformed architectures, while less rigid polyamine-macrocycles have been obtained by combining the rigidity of the terpyridine group with the flexibility of aliphatic polyamine chains. To offer a more comprehensive assessment of these ligands, also the properties of terpyridine, as the basic motif of this review, are also briefly described.

2. Terpyridine

Assuming that the three rings of terpyridine prefer a planar geometry to achieve maximum conjugation, three conformations of the molecule are possible, namely the *trans*,*trans*, *trans*,*cis* and *cis*,*cis* conformations, as depicted in Fig. 1. Quantum mechanics calculations performed on the free molecule have shown that the order of energies for these conformations is *trans*,*trans* < *trans*,*cis* < *cis*,*cis*, this conformational preference being caused by steric repulsion between 3,3′ and 3″,5″ hydrogen atoms, respectively, and possibly by electron–electron repulsion between the lone pairs on the nitrogen atoms [89].

This result is consistent with two crystal structures of terpyridine, showing the molecule in a nearly coplanar *trans*,*trans* conformation [90,91], and with ^{1}H NMR studies [92–95] and UV spectroscopy [96,97] in solution, although free terpyridine in the *cis*,*cis* conformation was found in the crystal structure of a stannacarborane complex in the absence of any evident intermolecular interaction contributing to stabilize this form [98]. Calculations showed that the *cis*,*cis* conformation could be stabilized in polar solvents by the formation of intermolecular hydrogen bonds. For instance, the hydrogen-bonded terpyridine–H_2O adduct shown in Fig. 2 is more stable by 11.29 kcal/mol than terpyridine and H_2O separated at infinity [89] and, accordingly, this structure was observed in the solid state [99–101].

Terpyridine undergoes protonation in moderately acidic solution giving rise to $[Htpy]^+$ and $[H_2tpy]^{2+}$ species, the successive protonation constants in water ($I = 0.1$ M, 298 K) being $\log K_1 = 4.7$ and $\log K_2 = 3.5$, respectively [102]. Depending on the protonation site and the molecular conformation, seven structures are possible for $[Htpy]^+$ (Fig. 3). Quantum mechanical calculations showed that the lowest energy structure in the gas phase is H(*c*,*c*-tpy)2 in which the protonated nitrogen of the central pyridine can form two hydrogen bonds with the nitrogen atoms of the lateral pyridines, while the highest energy structures are H(*t*,*t*-tpy)1 and H(*t*,*t*-tpy)2 whose conformations prevent the formation of intramolecular hydrogen bonds, leading

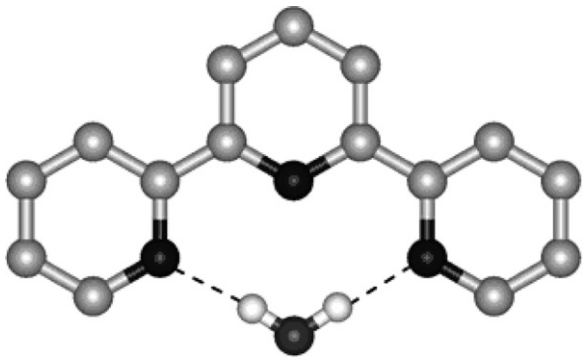

Fig. 2. The *cis*,*cis* conformation of terpyridine stabilized by hydrogen bonds with a water molecule.

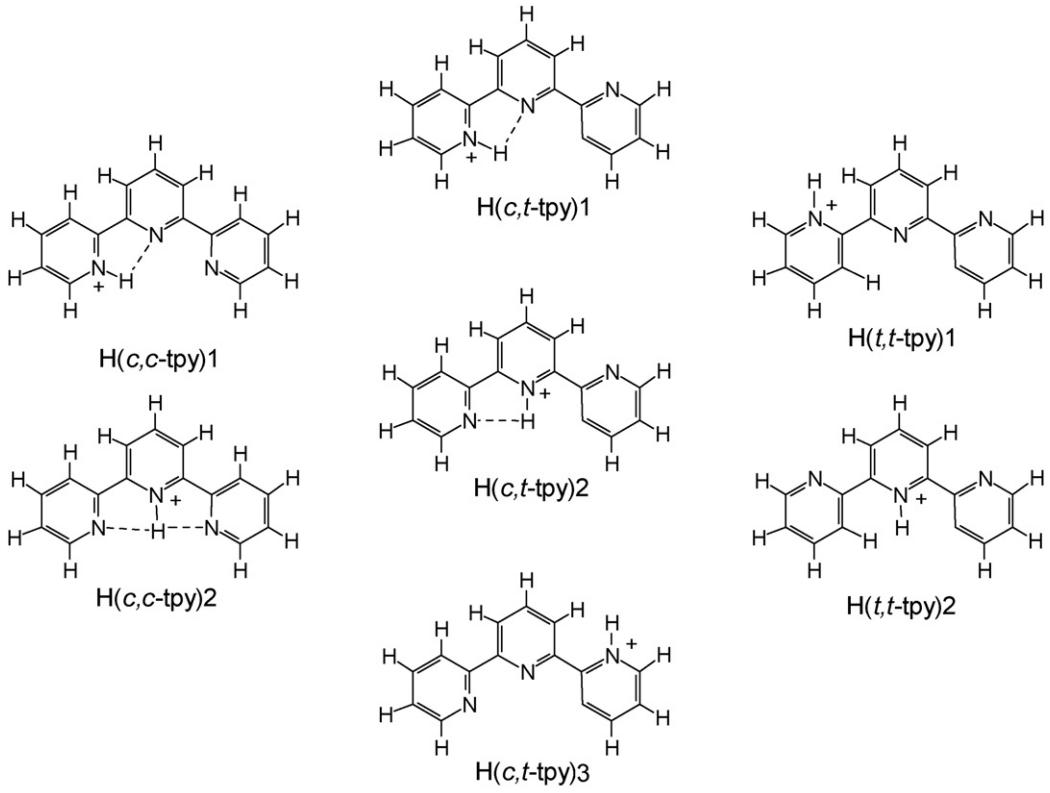

Fig. 3. The seven possible structures of the $[Htpy]^+$ cation.

instead to intramolecular H···H repulsion between *cis* N–H and C–H groups [89]. In the crystal structure of $[Htpy][CF_3SO_3]$, however, the monoprotonated $[Htpy]^+$ cation shows the H(*c,t*-tpy)1 structure and forms an additional hydrogen bond with the $CF_3SO_3^-$ anion [103]. Hence, taking into account the ability of the H(*c*,*t*-tpy)1 form to interact with the medium, it was concluded that in the presence of solvents and/or anions which can accept hydrogen bonds, this structure is more likely to be found than that of H(*c*,*c*-tpy)2 despite this having lower energy in the gas phase [89].

For the diprotonated $[H_2tpy]^{2+}$ species different structures are also possible. As found for the monoprotonated species, quantum mechanics calculations [89] again showed that in the gas phase also for $[H_2tpy]^{2+}$ the lower energy structures are stabilized by intramolecular hydrogen bonds, while unfavourable contributions due to N–H···C–H repulsions are responsible for the higher energy ones. The lowest energy structure of $[H_2tpy]^{2+}$ has a *cis*,*cis* conformation, with the two acidic protons on the lateral pyridine groups, leading to the formation of two intramolecular hydrogen bonds (Fig. 4a). This conformation was also observed in two crystal structures where the $[H_2tpy]^{2+}$ cations are further stabilized by a couple of strong hydrogen bonds with encapsulated water molecules or nitrate anions (Fig. 4b and c) [89]. Optimisation of the lowest energy structure with an encapsulated water molecule gave an energy for the adduct lower by 18.72 kcal/mol than that of $[H_2tpy]^{2+}$ and H_2O separated at infinity, thus leading to the conclusion that in the case of the diprotonated terpyridine species the gas phase preference for the *cis*,*cis* structure is enhanced in water where it is likely to be the only diprotonated species present [89].

The ultraviolet spectrum of terpyridine in aqueous solution is strongly pH dependent (Fig. 5) [96]. In alkaline solution, where terpyridine is present as a free base in the *trans*,*trans*

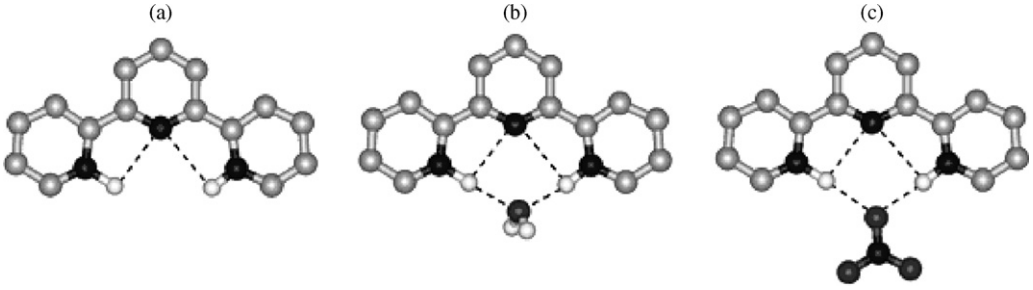

Fig. 4. Schematic structures of $[H_2tpy]^{2+}$ (a), $[H_2tpy(H_2O)]^{2+}$ (b) and $[H_2tpy(NO_3)]^+$ (c).

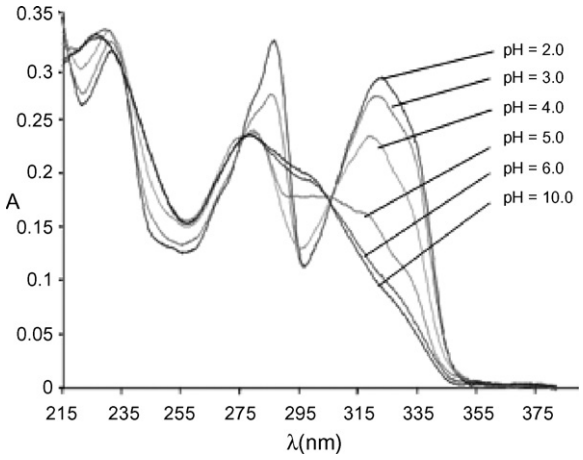

Fig. 5. UV spectra of terpyridine at different pH values.

conformation, the spectrum consists of two bands at 285 and 235 nm ($\varepsilon = 16{,}000$ and 19,500 $mol^{-1}\ dm^3\ cm^{-1}$, respectively, at pH 12) and is very similar to those in organic solvents. As the solution pH is decreased to intermediate values, a new spectrum consisting of three bands at *ca*. 320, 279 and 232 nm ($\varepsilon = 14{,}000$, 14,500 and 19,000 $mol^{-1}\ dm^3\ cm^{-1}$, respectively, at pH 4) appears, corresponding to the formation of the monoprotonated *cis*,*trans* $[Htpy]^+$ species, occurring at intermediate pH values. Further protonation, leading to the formation of the *cis*,*cis* $[H_2tpy]^{2+}$ species in more acidic solution, gives rise to some modifications of the spectrum observed at an intermediate pH. Although the three bands undergo only modest wavelength shifts to *ca*. 325, 285 and 230 nm, their molar extinction coefficients increase appreciably ($\varepsilon = 18{,}000$, 20,500 and 18,000 $mol^{-1}\ dm^3\ cm^{-1}$, respectively, at pH 1.8) and the 325 and 285 nm bands show poorly resolved fine structure (Fig. 5).

The fluorescence spectrum of terpyridine is also markedly pH dependent [105]. In alkaline solution the emission spectra are characterized by a band resulting from the overlapping of two peaks at 337 and 350 nm. This band becomes more intense and is red-shifted on lowering the solution pH, as the $[Htpy]^+$ and $[H_2tpy]^{2+}$ species are formed. The intensity of the 350 nm band was found to increase with acid concentration up to 2.35 M H_2SO_4 possibly due to protonation of the third pyridine group in very acidic media. The shorter wavelength emission occurring in basic media indicates that the molecule has enhanced proton affinity in the excited state with respect to the ground state. The fluorescence quantum yields at 300 K for three representative conditions are $\phi = 0.11$ in 0.1 M NaOH, $\phi = 0.27$ in pure water and $\phi = 0.61$ in 0.05 M H_2SO_4. A photophysical study of terpyridine in different solvents at 300 K showed that while the free base deactivates mostly *via* non-radiative routes its protonated forms prefer radiative processes [105].

In general, terpyridine acts as a terdentate ligand forming metal complexes in which it assumes the *cis*,*cis* conformation. The most typical coordination motif of terpyridine is represented by the $[M(tpy)_2]^{2+}$ complexes in which two nearly planar terpyridine ligands are almost perpendicular to each other around

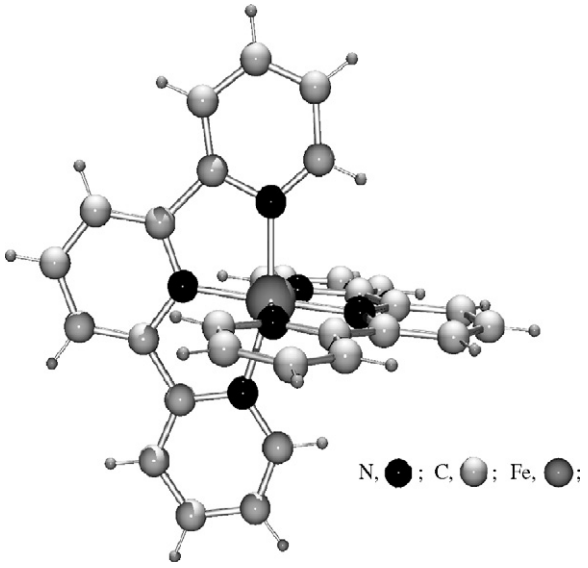

Fig. 6. Crystal structure of the $[Fe(tpy)_2]^{2+}$ complex cation [106].

the metal ion and define a distorted octahedral coordination of approximate D_{2d} symmetry. A characteristic of these structures is compression along the axis defined by the central rings of the two-terpyridine groups due to the small bite of terpyridine in octahedral coordination (Fig. 6). In the case of metal ions subjected to Jahn–Teller effects in octahedral coordination, like Cu(II), an elongation takes place along one of the two directions perpendicular to the previous axis leading to a coordination polyhedron with C_{2v} symmetry [107].

The configuration of the 1:2 metal complexes, in which the two-terpyridine molecules are perpendicular to each other, leads the hydrogen atoms in 6 and 6″ positions being located above the plane of the central aromatic ring of the adjacent terpyridine (Fig. 6). As a consequence of this structural feature the ^1H NMR signal of these unique protons undergoes a large upfield shift, with respect to the free ligand, which is characteristic of 1:2 complexes [87,92,93]. Indeed, as shown in Fig. 7 for $[Zn(tpy)]^{2+}$, in the case of 1:1 complexes a similar displacement is not observed for the signal of the 6,6″-protons which instead moves downfield upon coordination.

Table 1 gives some stability constant values for terpyridine metal complexes [102]. The stability of the 1:1 complexes follows the order expected for high spin octahedral complexes,

Table 1
Protonation and metal complexation constants of terpyridine determined in aqueous solution

Ion	$\log K_1$	$\log K_2$
H^+	4.7	3.5
Mn^{2+}	4.44	
Fe^{2+}	7.1	13.6
Co^{2+}	9.5	9.1
Ni^{2+}	10.7	11.1
Cu^{2+}	12.3	6.8
Zn^{2+}	6.0	
Cd^{2+}	5.1	

$I = 0.1$ M, $T = 298$ K [102].

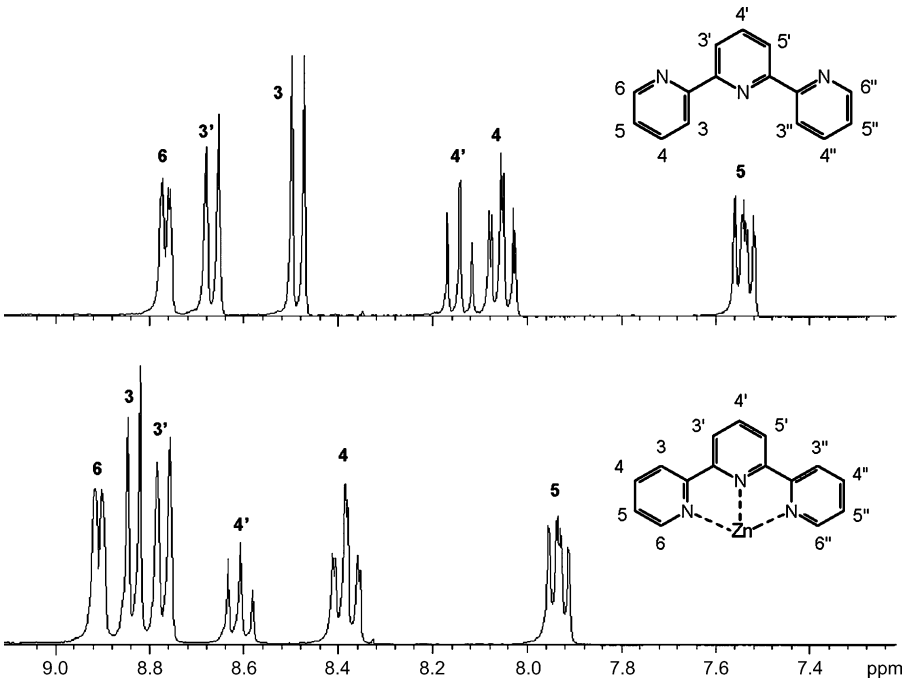

Fig. 7. ^{1}H NMR spectra of terpyridine (top) and $[Zn(tpy)]^{2+}$ and (bottom) in DMSO [104].

increasing from Mn(II) to Cu(II) and decreasing from Cu(II) to Zn(II). In general the equilibrium constant for the binding of the second terpyridine molecule, to form 1:2 complexes, is smaller than the constant for the formation of 1:1 species. In the case of Cu(II) the second binding constant is noticeably smaller owing to the Jahn–Teller effect leading to longer binding distances (weaker coordination bonds). In contrast, with Fe(II), the equilibrium constant for the binding of the second terpyridine molecule is considerably greater than the constant for the binding of the first one in agreement with the formation of a very stable d^6 low spin $[Fe(tpy)_2]^{2+}$ complex. The d^7 $[Co(tpy)_2]^{2+}$ complex was reported to exhibit room temperature equilibrium between low spin ($S = 1/2$) and high spin ($S = 3/2$) electronic states [108].

The ultraviolet spectra of terpyridine complexes are similar to that of the metal-free ligand in acidic solutions. All these compounds exhibit three bands at about 320–340, 270–285 and 220–235 nm although resolution of the satellite bands depends on the metal ion [96]. As an example the UV spectrum of $[Zn(tpy)]^{2+}$ is reported in Fig. 8 along with that of protonated terpyridine.

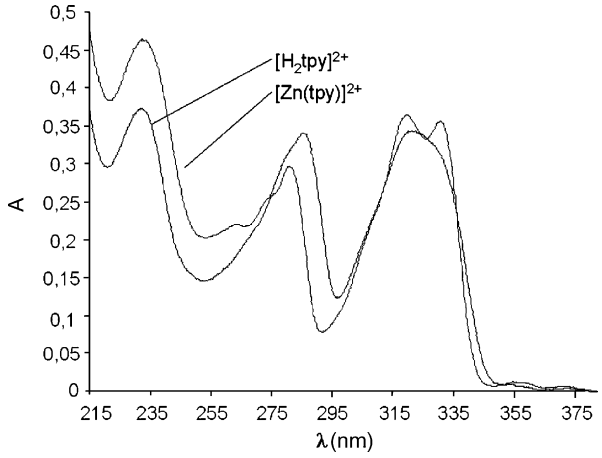

Fig. 8. UV spectra of $[H_2tpy]^{2+}$ and $[Zn(tpy)]^{2+}$.

3. Schiff-base macrocycles

The first macrocyclic ligands containing a terpyridine group **1** was synthesised by template condensation of 6,6′-

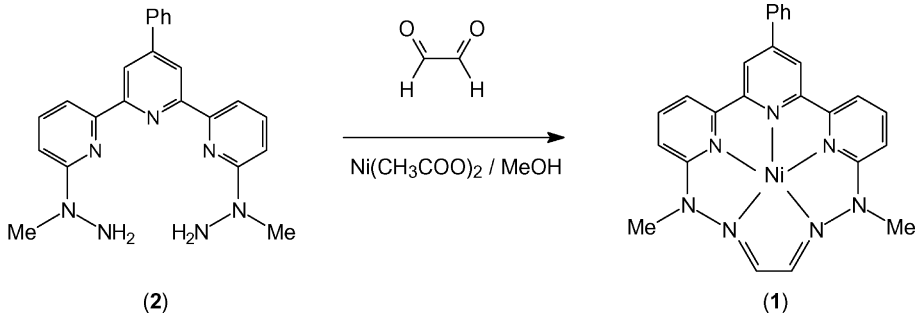

Fig. 9. Template synthesis of $[Ni(\mathbf{1})]^{2+}$.

bis(methylhydrazino)-4′-phenyl-2,2′:6′,2″-terpyridine **2** with glyoxal in the presence of $Ni(OAc)_2{\cdot}4H_2O$ in refluxing methanol (Fig. 9) and isolated as the $[Ni(\mathbf{1})(MeOH)_2][BF_4]_2$ complex upon addition of $[n\text{-}Bu_4N][BF_4]$ to the resulting solution [109]. This condensation, leading to a metal complex, only proceeded satisfactorily by using Ni(II) or Mn(II) as the template ions, while attempts to perform the same reaction in the presence of Ba(II), Ca(II), Sr(II), Cd(II), Zn(II), Hg(II), Rh(II), Ru(II), Fe(II), Co(II), or Cu(II) were unsuccessful. However, excellent yields of the free ligand, isolated as $[H_2(\mathbf{1})][PF_6]_2$ were obtained when the condensation was performed in the presence of $CrCl_3{\cdot}6H_2O$ [110].

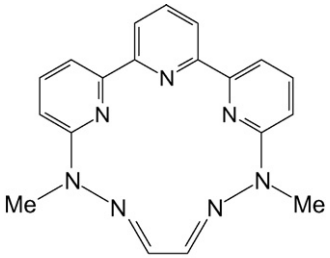

(**3**)

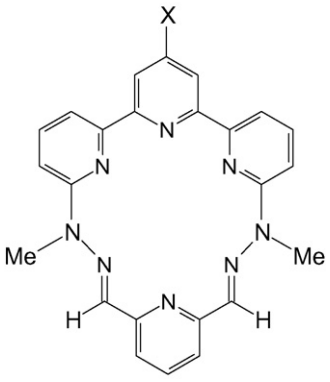

X = H, (**4**) X = Ph, (**5**)

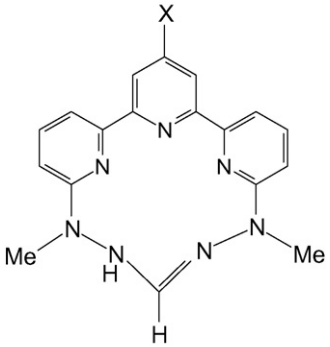

X = H, (**6**) X = Ph, (**7**)

The crystal structures of the complexes $[Ni(\mathbf{1})(EtOH)_2][BF_4]_2$ [110], $[Co(\mathbf{1})(imidazole)_2][PF_6]_2{\cdot}(CH_3)_2CO$ [111] and $[Cu(\mathbf{1})(imidazole)_2][PF_6]_2$ [112] were solved by means of X-ray diffraction. These showed the metal ions to be in pentagonal bipyramidal coordination environments defined by five nitrogen donors of the macrocycle in equatorial positions and two ethanol molecules, in the case of Ni(II), or two imidazole molecules, in the case of Co(II) and Cu(II), in the axial sites (Fig. 10). The five equatorial donors and the metal ion in each structure are coplanar; for instance the maximum deviation from the least-squares plane is 0.01 Å in the Ni(II) complex. The two uncoordinated nitrogen atoms of the macrocycle have a planar geometry; they are sp^2 hybridized and essentially coplanar with the above least-squares plane.

The metal ions are displaced towards the pyridine-N donors, especially that of the central pyridine. This feature was attributed to a π-type interaction between the metal atom and the central pyridine ring [110]. The positive charge of the metal ion favours conjugation of the 4′-phenyl substituent with the ring, thus increasing the multiple-bond character of the metal-N bond.

The preparation of the metal-free ligand was also successfully achieved by a transient template reaction involving dimethyltin(IV) [110]. Reaction of **2** with $SnMe_2Cl_2$ in chlorobenzene, 1,2-dichloroethane, or chloroform, gave rise to the $[SnMe_2(\mathbf{2})]Cl_2$ complex. Condensation of this complex with glyoxal in methanol in the presence of a trace of acid afforded the solid $[H_2(\mathbf{1})][PF_6]_2$ on addition of $[NH_4][PF_6]$, after removal of SnO_2 formed upon demetallation of the macrocycle. The crystal structure of the diprotonated ligand salt (Fig. 11) showed the macrocyclic ring in a conformation very similar to those observed in its metal complexes with the terpyridine group in the *cis*,*cis* conformation and having essentially planar geometry, the maximum deviation from the least squares plane through the15 atoms defining the ring being 0.04 Å. Hole-size calculations based on the circle described by the five donor atoms showed no significant differences between this structure and the structure of the Ni(II) complex, 2.12 Å for the free macrocycle and 2.10 Å for the complex [110]. The structural parameters (bond distances and angles) of the diprotonated ligand indicate that the macrocycle is a delocalised systems.

As shown by the molecular structures of **1** in its metal complexes and metal-free form, the macrocycle behaves as a shape-persistent donor system imposing a planar pentagonal coordination environment on metal ions, which achieve a pentagonal-bipyramidal geometry by addition of two further ligands in apical positions. This happens even for metal ions, such as Ni(II) and Cu(II), for which hepta-coordination is a rare event.

The attainment of the metal-free macrocycle from the reactions in the presence of Cr(III) and dimethyltin(IV) was unexpected. The "transient template effect" shown by Cr(III) was firstly ascribed to the unfavourable planar pentagonal or pentagonal bipyramidal coordination geometries imposed by **1** on this d^3 metal ion, which prefers an octahedral environment [110]. Complexes of this metal ion, however, are known to be stable to demetallation. For this reason, further studies on this Cr(III)-mediated effect were performed, showing that the true template in these reactions is the proton. The sole function of Cr(III) is to provide a source of protons through the hydrolysis of coordi-

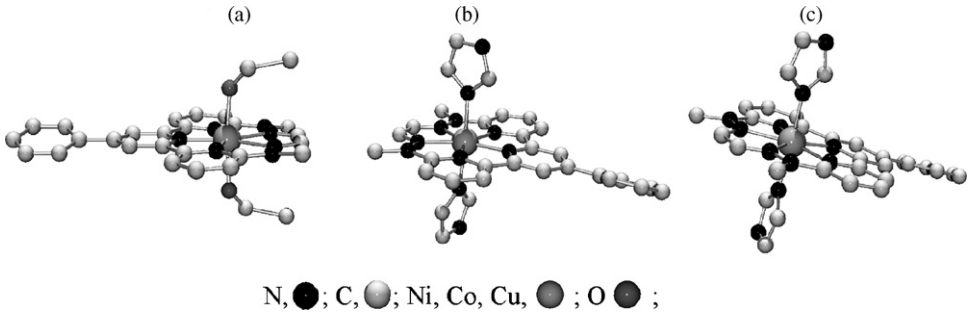

Fig. 10. Structures of (a) $[Ni(\mathbf{1})(EtOH)_2]^{2+}$, (b) $[Co(\mathbf{1})(imidazole)_2]^{2+}$ and (c) $[Cu(\mathbf{1})(imidazole)_2]^{2+}$ complex cations.

nated water molecules [113]. In the case of dimethyltin(IV), the observed transient template effect was ascribed to a dimensional mismatch between the metal and the macrocyclic cavity. This hole-size mismatch must arise from the particular N_5 donor set of **1**. As shown by the crystal structure of the $[SnMe_2(\mathbf{2})][PF_6]Cl$ complex [114], the Sn atom has a pentagonal bipyramidal coordination geometry with five nitrogen donor of **2** in equatorial position and two methyl groups in the apical sites. The hole size of this open-chain ligand is 2.32 Å, which is considerably larger than that of the macrocycle. Hence, the reduction in hole size occurring on passing from the open-chain ligand **2** to the macrocycle **1** enhances the lability of the dimethyltin(IV) giving a local kinetic contribution to this transient template effects whose ultimate origin, the formation of insoluble tin dioxide, is thermodynamic in nature. Furthermore, the formation of the $[H_2(\mathbf{1})]^{2+}$ species competes with the metal complexes favouring demetallation.

Ligand **1**, thanks to its π-acceptor properties, stabilizes the low oxidation state Ni(I) d^9 cation, as shown by the electrochemical study of the bis-acetonitrile adduct $[Ni(\mathbf{1})(CH_3CN)][BF_4]_2$ [109]. Cyclic voltammetry of this compound in acetonitrile revealed two reversible one electron reduction waves at $^1E_{1/2} = -1.07$ V and $^2E_{1/2} = -1.49$ V (versus Ag-$AgNO_3$ reference electrode). The dark green Ni(I) complex is generated at the first reduction potential, as confirmed by the EPR spectrum of the solution obtained by means of controlled potential electrolysis of the yellow $[Ni(\mathbf{1})(CH_3CN)][BF_4]_2$ complex in acetonitrile. On the other hand, reduction of the complex at the second potential yielded a mauve solution, the EPR spectrum of which showed the formation of a Ni(I) ligand radical species with two essentially discrete paramagnetic centres, the second electron residing on the macrocycle [109]. The electrochemical behaviour of a series of heptacoordinated complexes $[Ni(\mathbf{1})X_2]^{2+}$ (X = 4-substitute pyridines, pyrazine, thiazole, imidazole, 1-methylimidazole, 2-methylimidazole, 1,2-dimethylimidazole, triphenylphosphite, dimethylsulfoxide and dabco) was studied by cyclic voltammetry in acetonitrile, showing for all complexes a one-electron reversible reduction wave in the range from −1.08 to −1.46 V versus Ag-$AgBF_4$ reference electrode due to ligand-centred processes [115]. Similar studies were also performed for the analogous Fe(II) [116], Mn(II) [117], Co(II) [111] and Cu(II) [112] complexes showing that also in the case of Fe(II) and Mn(II) species the observed reduction reactions in acetonitrile take place on the ligand, while Co(I) and Cu(I) complexes are generated upon reduction in DMSO. In the case of the Ag(I) complex, a ligand radical species is probably the product of a one-electron reversible process occurring at +0.75 V (versus Ag-$AgBF_4$) in acetonitrile, although definitive evidence for this was not obtained [118].

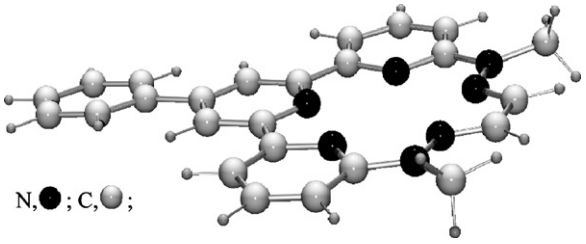

Fig. 11. Crystal structure of the $[H_2(\mathbf{1})]^{2+}$ cation.

The unsubstituted ligand **3**, analogous to **1**, was later synthesised in the metal-free form by a transient template reaction with dimethyltin(IV) and isolated as $[H_2(\mathbf{3})][PF_6]_2$ [119]. Metal complexes $[M(\mathbf{3})(H_2O)_2][PF_6]_2$ with M = Co(II), Ni(II), Cu(II) and Zn(II) were prepared for which pentagonal bipyramidal coordination geometries with the water molecules in apical positions were proposed. The ^1H NMR spectrum of the Zn(II) complex closely resembles that of $[H_2(\mathbf{3})][PF_6]_2$ indicating that both species contain the ligand in almost the same conformation.

The electrochemical behaviour of the Co(II), Ni(II) and Cu(II) complexes was analysed in acetonitrile after conversion of $[M(\mathbf{3})(H_2O)_2][PF_6]_2$ into the corresponding acetonitrile $[M(\mathbf{3})(CH_3CN)_2][PF_6]_2$ complexes [119]. Cyclic voltammetry of $[Co(\mathbf{3})(CH_3CN)_2][PF_6]_2$ in acetonitrile showed a reversible oxidation wave at +1.102 V and a quasi-reversible reduction at −1.340 V (versus Ag-Ag(I)(acetonitrile) reference electrode). The oxidation process, corresponding to the formation of the Co(III) complex, is analogous to that found for the phenyl substituted complex $[Co(\mathbf{1})(CH_3CN)_2][PF_6]_2$ occurring at +1.11 V. The oxidation wave disappeared upon addition of π-acceptor ligands (CO, $P(OMe)_3$), while two reduction waves developed: one reversible at −1.250 V and one irreversible at −1.8 V. Similarly, the $[Co(\mathbf{1})(CH_3CN)_2][PF_6]_2$ complex exhibits a reversible reduction wave at −1.36 V, which moves

to −1.24 V in the presence of π-acceptor ligands. Reduction of $[Co(\mathbf{3})(CH_3CN)_2][PF_6]_2$ and $[Co(\mathbf{1})(CH_3CN)_2][PF_6]_2$ in the absence of added π-acceptor ligands at the first reduction potentials, performed by means of controlled potential electrolysis in acetonitrile, led to green solutions whose EPR spectra revealed the formation of ligand-centred radicals of the Co(II) complexes, while Co(I) complexes are generated in the presence of π-acceptor ligands. Reduction of $[Co(\mathbf{3})(CH_3CN)_2][PF_6]_2$ at the second potential in the presence of π-acceptor ligands resulted in the formation of the Co(I) complex $\{Co^{I}(CH_3CN)_2[(\mathbf{3})^{\bullet -}]\}^0$ containing the ligand in reduced radical form.

The $[Ni(\mathbf{3})(CH_3CN)_2][PF_6]_2$ complex showed rather different electrochemical features to those of $[Ni(\mathbf{1})(CH_3CN)_2][PF_6]_2$, indicating a significant contribution of the 4′-phenyl substituent in stabilizing the Ni(I) metal centre. Indeed, cyclic voltammetry of the Ni(II) complex of **3** in acetonitrile revealed a quasi-reversible oxidation at +1.09 V, a quasi-reversible reduction at −1.5 V and an irreversible one at −1.5 V, in contrast to the two fully reversible reductions exhibited by $[Ni(\mathbf{1})(CH_3CN)_2][PF_6]_2$. Even in the presence of a π-acceptor ligand, full reversibility of the reduction processes of $[Ni(\mathbf{3})(CH_3CN)_2][PF_6]_2$ was not achieved, and all attempts to electrogenerate a Ni(I) complex under different conditions were unsuccessful. A similar effect of the 4′-substituents in stabilizing the low oxidation state of the metal was previously observed for the first transition metal complexes with phenyl-substituted terpyridines [120,121]. Delocalization of the electron density of the Ni(I) ion on the aromatic groups, with increased multiple-bond character of the Ni–N bond and extension of the conjugation to the phenyl ring, is most likely one of the principal contributions to such an effect, along with the protection that the bulky phenyl substituent gives towards dimerization of the radical species occurring through the 4′ position.

The cyclic voltammogram of the orange–brown $[Cu(\mathbf{3})(CH_3CN)_2][PF_6]_2$ complex in acetonitrile showed three waves corresponding to one quasi-reversible oxidation, one quasi-reversible reduction and one irreversible reduction processes [119]. The quasi-reversible oxidation occurring at +1.20 V becomes fully reversible at 77 K and was ascribed to the formation of the Cu(III) complex. The quasi-reversible reduction occurring at −0.31 V gave rise to the corresponding Cu(I) complex, in agreement with the formation of a diamagnetic solution upon controlled-potential reduction of the Cu(II) complex and with the observed changes in the electronic spectrum.

Template reactions similar to those employed for the synthesis of **1** and **3**, performed in the presence of Ni(II) and 2,6-pyridinedialdehyde, afforded the hexadentate macrocycles **4** and **5** either as free ligands or as Ni(II) complexes depending on the reaction conditions [122].

It was found that the free ligands were only obtained if the reaction solutions were moderately concentrated and strongly acidic in HCl, while in diluted or slightly acidic solutions the products were the Ni(II) complexes. The formation of the free ligands in these reactions was rather surprising, but the identity of the two products was unambiguously established. All experimental evidences were consistent with a template action of Ni(II) also for reactions leading to the metal-free ligands, and an acid catalysed demetallation, aided by the specific action of chloride through the formation of $[NiCl_4]^{2-}$, was proposed as the key step of these processes. The estimated hole size of these macrocycles was about 2.7 Å, which means that the stability of the complex cannot be high due to a mismatch with the metal ion size, thus favouring the complex demetallation.

Attempts to prepare **4** and **5** via transient template reactions in the presence of dimethyltin(IV) did not provide the expected dimethyltin(IV) complexes with these macrocycles. Indeed, characterization of the new compounds strongly suggested that a metal ion induced rearrangement led to the formation of the dimethyltin(IV) complexes with the pentadentate macrocycles **6** and **7** [122]. Although it was not possible to obtain the free macrocycles from the tin complexes, it was reported that transmetallation occurs readily upon treatment with other transition metal ions [122].

Many other Schiff-base aza-macrocycles, not containing terpyridine, have been synthesised and used for metal ion complexation. A variety of ligand structures, both macrocyclic and macrobicyclic, frequently bearing additional coordinating functionalities in lateral chains, has been achieved by changing the number of imine nitrogen atoms and/or by incorporating different coordinating groups such as pyridine, bipyridine, pyridazine, phenol and thiophenol, among others [123–126].

Among Schiff-base polyamine-macrocycles, those containing terpyridine, described in this section, are characterized by a greater molecular rigidity. A consequent distinctive properties of these ligands is their ability to impose a preformed arrangement of donor atoms to coordinated metal ions, which are forced into uncommon coordination spheres. As shown above, uncommon properties of metal complexes are frequently with their special structures.

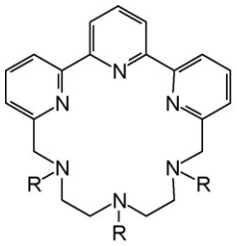

R = CH_2COOH, (**8**)
R = H, (**9**)
R = Ts, (**10**)
R = CHCOOtBu, (**12**)

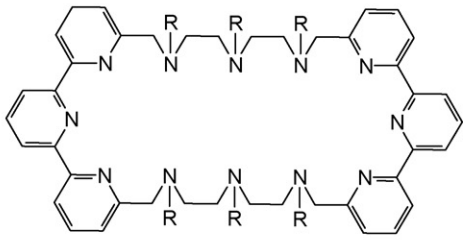

R = Ts, (**11**)
R = CHCOOtBu, (**13**)

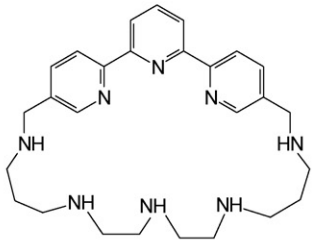

(**14**)

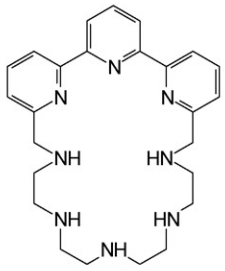

(**15**)

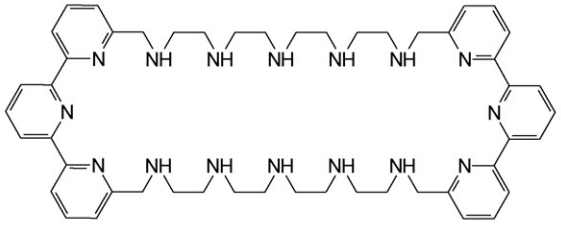

(**16**)

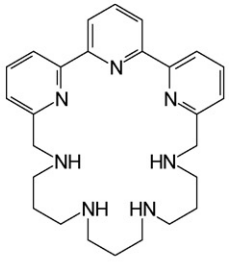

(**17**)

4. Polyamine-macrocycles

The triaza-triacetate macrocycle **8**, containing a terpyridine moiety as part of its ring, was synthesised in order to obtain a ligand forming stable luminescent complexes with lanthanide cations (Eu(III), Tb(III), Sm(III), Dy(III)) [127,128]. The first synthetic strategy intended to obtain **8** through the functionalization of the intermediate macrocycle **9**, prepared according to a modified Richman and Atkins method [129] involving the reaction of 1,4,7-tritosyl-1,4,7-triazaheptane with 6,6″-bis-bromomethyl-[2,2′:6′,2″]-terpyridine and successive removal of tosyl groups from the cyclization product **10**. However, this procedure did not give the desired compound, but mainly the dimeric 36-membered macrocycle **11**. The target compound was successfully obtained by means of a metal template reaction involving 1,4,7-tri*tert*butoxicarbonylmethyl-1,4,7-triazaheptane and 6,6″-bis-bromomethyl-[2,2′:6′,2″]-terpyridine in acetonitrile in the presence of Na_2CO_3, affording the cyclic derivative **12**

which was subsequently converted to **8** by treatment with trifluoroacetic acid. When the same reaction was performed using Li_2CO_3, the macrocycle **12** was also obtained but along with larger amounts of polymeric materials, while the same reaction using K_2CO_3 yielded the dimeric compound **13**.

The Eu(III) and Tb(III) complexes with **8**, which are nine-coordinated by ligand donors, showed exceptional luminescence properties (high decay time, quantum yield, and excitation wavelength) in aqueous solution and appeared to be highly interesting as luminescent biolabels. In contrast, the Sm(III) and Dy(III) complexes displayed very poor luminescence quantum yields [127,128].

Synthetic procedures based on the Richman and Atkins method [129] were successful in affording the polyamine-macrocycles **14**, **15**, **16**, and **17** [75,130,131]. Ligands **15** and **16** are 1:1 and 2:2 condensation products isolated from the one cyclization reaction [130].

The two octa-aza ligands **14** and **15** differ in that **14** has two propylene instead of two ethylene spacers, and in that the polyamine chain is attached at 5,5″ for **14** and 6,6″ for **15**. The consequences of these differences are not trivial, and **14** and **15** have quite different metal-binding properties, especially in regard to substrates activation [75–77,130].

The basicity and coordinating strength of **14**, **15** and **17** were studied by various techniques [75–77,130,131]. Their distinctive properties reflect the presence in their structures of the two different binding moieties, namely the terpyridine group displaying low basicity and good metal binding ability, and the polyamine chain characterized by high basicity and high affinity for metal ions. Accordingly, protonation of these macrocycles occurs on the polyamine chain from alkaline to fairly acidic pH, while terpyridine undergoes protonation only in very acidic solutions. Table 2 reports the protonation constants of **14**, **15** and **17** determined by means of potentiometric titrations in aqueous solution [76,130,131].

As for free terpyridine, the UV spectra are particularly sensitive to protonation also for this type of ligands. In particular, modification of the band at about 290 nm is diagnostic for the protonation of the heteroaromatic nitrogen atoms. Indeed, splitting of this band with formation of a new one at about 325–335 nm was found to accompany the last protonation steps

Table 2
Protonation constants of (**14**) [76], (**15**) [130] and (**17**) [131] in aqueous solution at 298.1 K

	log *K*		
	(**14**)[a]	(**15**)[b]	(**17**)[b]
$L + H = HL$[c]	9.21	9.31	10.99
$HL + H = H_2L$	8.17	8.63	8.68
$H_2L + H = H_3L$	7.04	7.27	7.36
$H_3L + H = H_4L$	5.74	3.92	6.36
$H_4L + H = H_5L$	3.82	2.80	1.81
$H_5L + H = H_6L$	3.27	2.10	

[a] $NaClO_4$ 0.15 M.
[b] NMe_4Cl 0.10 M.
[c] Charges omitted.

of all three ligands indicating that terpyridine protonation takes place at those stages [76,130,131]. As an example, the pH dependence of the absorption spectrum of **15** is reported in Fig. 12a.

^1H NMR and fluorescence spectroscopic measurements confirmed this feature [130,131]. Typically, the fluorescence emission of the free ligands is enhanced on lowering the solution pH, as shown for **15** in Fig. 12b, because protonation of the amine groups prevents the emission quenching occurring *via* electron transfer from the nitrogen lone pairs. In the most emissive species, all the aliphatic amine groups are protonated. Protonation of terpyridine leads, in this case, to a decrease of the fluorescence emission due to the mixing of the n–π* excited states with the π–π* ones, thus lowering the fluorescence quantum yield.

As a consequence of the basicity properties of these ligands, highly protonated forms of their complexes and protons bound to the aliphatic amino sites, are formed in very acidic solutions.

The 5,5″ attachment of the aliphatic chains to terpyridine in **14**, means that metal ions coordinated to the terpyridine site are not able to interact with the amine groups in benzylic positions. Hence, the propylenic chains separate two distinct binding units where two metal ions can be accommodated at a sufficiently long distance to host bridging substrates. This is seen in the crystal structure of the $\{Cu_2[H_2(\mathbf{14})](CO_3)(ClO_4)_2\}^{2+}$ complex cation (Fig. 13) in which two Cu(II) ions located 5.15 Å apart from each other bind a μ,μ′-bismonodentate car-

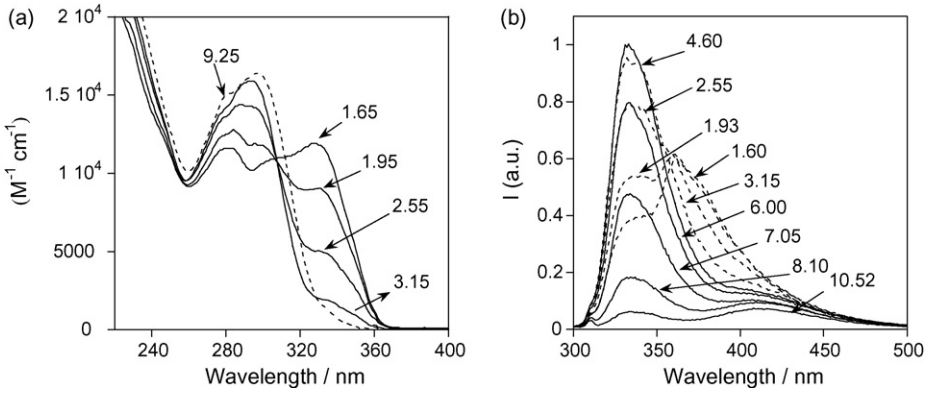

Fig. 12. Absorption and emission (λ_{exc} 282 nm) spectra of (**15**) in aqueous solution at various pH values. $[(\mathbf{15})] = 2.68 \times 10^{-5}$ M, 298 K. Reprinted in part with permission from Ref. [130]. Copyright 2004 American Chemical Society.

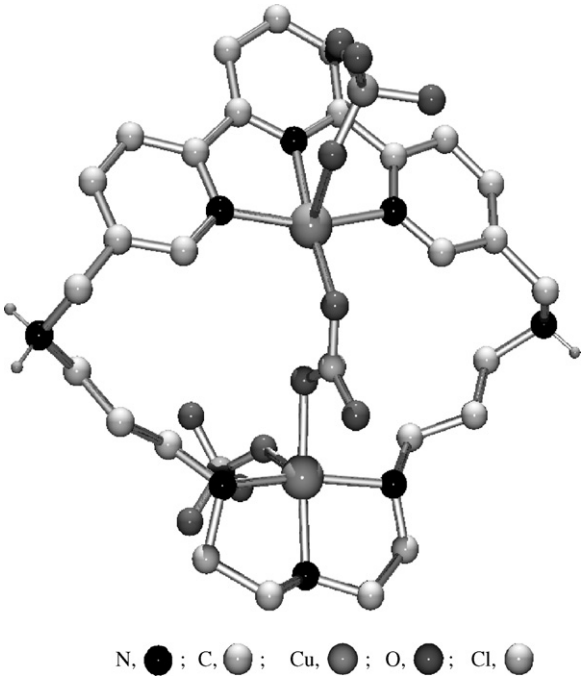

Fig. 13. Crystal structure of the $\{Cu_2[H_2(\mathbf{14})](CO_3)(ClO_4)_2\}^{2+}$ complex cation.

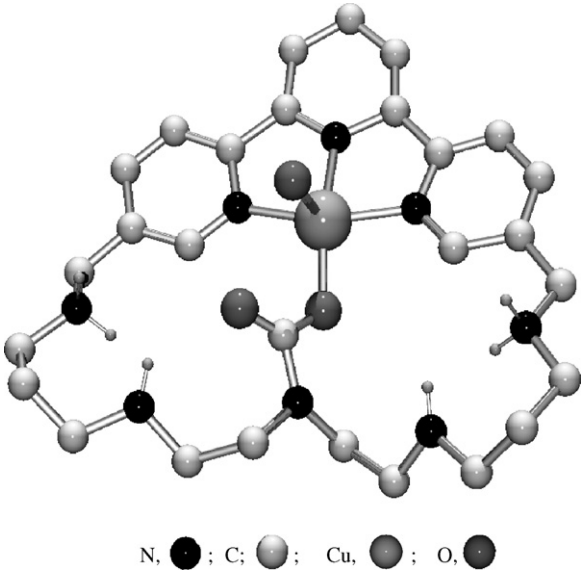

Fig. 14. Structure of the complex cation present in the crystal of $\{Cu[H(\mathbf{14})\text{-carbamate}](H_2O)\}(ClO_4)_3\cdot 2H_2O$.

bonate anion [75,76]. The Cu(II) ions show distorted square pyramidal coordination environments with perchlorate anion in apical positions. The two-amine groups in benzylic positions are protonated.

Interestingly, this carbonate complex formed spontaneously from the dicopper(II) complex of **14** upon absorption of atmospheric CO_2 in slightly alkaline (pH 9) solutions. The avidity of the Cu(II) complexes with **14** towards CO_2 was also manifested by the mononuclear complex. Indeed, exposure to the air of a solution containing $Cu(ClO_4)_2$ and **14**, in 1:1 molar ratio, at an initial pH of 9 led to a rapid acidification of the solution followed by crystallization of the $\{Cu[H(\mathbf{14})\text{-carbamate}](H_2O)\}(ClO_4)_3\cdot 2H_2O$ complex formed by metal-ion-assisted reaction of the central amine group of the chain with atmospheric CO_2 assisted by the metal ion. The crystal structure of the $\{Cu[H(\mathbf{14})\text{-carbamate}](H_2O)\}^{3+}$ complex cation is shown in Fig. 14. Again, the coordination geometry around Cu(II) can be described as a distorted square pyramid, its base being defined by the terpyridine nitrogen atoms and an oxygen atom of carbamate, while a water molecule occupies the apical position. The nitrogen atom involved in the formation of the carbamate loses one proton to form the N–C bond while two amine groups of the sides are protonated.

The ligand **14** is able to form mono-and binuclear complexes with Cu(II), as well as with Zn(II), also in aqueous solution [76]. The stability constants of $[Cu(\mathbf{14})]^{2+}$ ($\log K = 13.1$) and $[Zn(\mathbf{14})]^{2+}$ ($\log K = 6.9$) are very similar to those of the analogous complexes with terpyridine (Table 1), confirming that metal ions coordinated to the heteroaromatic nitrogen atoms do not interact with aliphatic amine groups. The binding of carbonate anion by the binuclear complexes and the formation of carbamate species in solution was studied by various techniques. The features of this CO_2 fixation from the atmosphere are similar to those of the enzyme rubisco, which participates in the fixation of CO_2 by green plants through the formation of a carbamate moiety assisted by Mg(II) or Mn(II) ions [132]. The ability of Cu(II) and Zn(II) complexes with **14** to uptake CO_2 is remarkable, since these complexes in solution rapidly absorb atmospheric CO_2 from the air, in contrast to other metal systems [133–136] requiring CO_2 bubbling to be efficient, and are able to do it even at physiological pH. Such properties can be correlated with the presence in the ligand of a terpyridine group, whose primary effect is to block a metal ion in a fixed position, without fulfill-

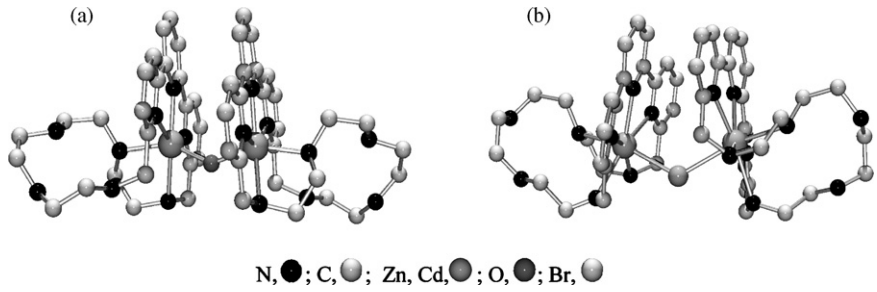

Fig. 15. Crystal structures of the $[\{Zn[H(\mathbf{15})]\}_2(\mu\text{-OH})]^{5+}$ (a) and $[\{Cd[H(\mathbf{15})]\}_2(\mu\text{-Br})]^{5+}$ (b) complex cations found in the solid state.

ing its coordination sphere, leading to more preorganized and efficient systems.

The octa-aza ligand **15** is more flexible than the analogous **14** in the binding of metal ions, using both the nitrogen atoms of the polyamine chain, including nitrogen atoms in benzylic positions, as well as the terpyridine donors [130]. Nonetheless, the ligand is not able to fully satisfy the coordination demands of metal ions, which are completed by exogenous ligands. In the crystal structures of the mononuclear Zn(II) and Cd(II) complexes (Fig. 15), the ligand is folded along the axis linking the benzylic carbon atoms, leaving an open zone on the metal ions where the additional ligands are coordinated. In these particular cases, intermolecular linkages through the formation of Zn–OH–Zn and Cd–Br–Cd bridges were observed. The resulting dimeric complexes are stabilized by the formation of face-to-face π-stacking interactions between the two almost parallel terpyridine moieties with an interplanar distance of 3.5 Å.

The coordination geometries of the two Zn(II) ions, which can be best described as distorted octahedrons, are very similar. Each Zn(II) is coordinated to the three heteroaromatic nitrogen atoms, two secondary nitrogen atoms of the same macrocyclic unit and the bridging hydroxide anion. The two secondary nitrogen atoms, one of which is a benzylic nitrogen, are only weakly bound to the metal ions. The Zn–Zn distance is 3.709 Å. The coordination geometries of the two Cd(II) ions are very similar also. Each Cd(II) ion is coordinated to three terpyridine nitrogen atoms, three secondary nitrogen atoms of the same macrocycle and the bridging bromide anion. The coordination geometry can be described as a distorted pentagonal bipyramid where the terpyridine nitrogen atoms and the benzylic amine groups define the equatorial plane, the bridging bromide anion and a further secondary nitrogen occupying the apical positions. One of the benzylic nitrogen atoms in the equatorial plane is bound at a longer distance than the remaining coordinated nitrogen atoms. The two Cd(II) ions are located 4.854 Å apart. While in the Zn(II) complex the pyridine units of terpyridine are almost coplanar, in the Cd(II) complex they display a larger deviation from coplanarity, with dihedral angles of 17.2°, between the pyridine planes comprising N3 and N2, and 14.5° between the planes comprising N10 and N11 (Fig. 15).

The most interesting feature of these dimeric complexes is the fact that they are assembled from monoprotonated $\{M[H(\mathbf{15})]\}^{3+}$ (M = Zn, Cd) units though the synergistic action of a bridging anion and the π-stacking interactions between the facing terpyridine groups. The resulting assemblies are characterized by high stability, in spite of the strong electrostatic repulsion between the 3+ charged monomeric units, as evidenced by the fact that the dimeric species with Zn(II) and the analogous ones with Cu(II) are also stable in aqueous solution [130]. In the case of Cu(II) the tendency to form dimeric complexes is higher than for Zn(II). In fact, while Zn(II) forms only the two dimeric complexes $[Zn_2H(\mathbf{15})_2]^{5+}$ (formulated above as $[\{Zn[H(\mathbf{15})]\}_2(\mu\text{-}OH)]^{5+}$) and $[Zn_2OH(\mathbf{15})_2]^{3+}$, which exists in equilibrium with the monomeric $\{Zn[H(\mathbf{15})]\}^{3+}$ species, in the case of Cu(II) monomeric species are not detected. The dimers $[Cu_2H_2(\mathbf{15})_2]^{6+}$, $[Cu_2H(\mathbf{15})_2]^{5+}$, $[Cu_2(\mathbf{15})_2]^{4+}$ and $[Cu_2OH(\mathbf{15})_2]^{3+}$ are the only detectable species above pH 3. Under more acidic conditions the dimeric species $[Cu_2H_2(\mathbf{15})_2]^{6+}$ disappears giving rise to the binuclear $[Cu_2(\mathbf{15})]^{4+}$ complex. The binuclear hydroxylated $[Zn_2OH(\mathbf{15})]^{3+}$ complex is formed by Zn(II).

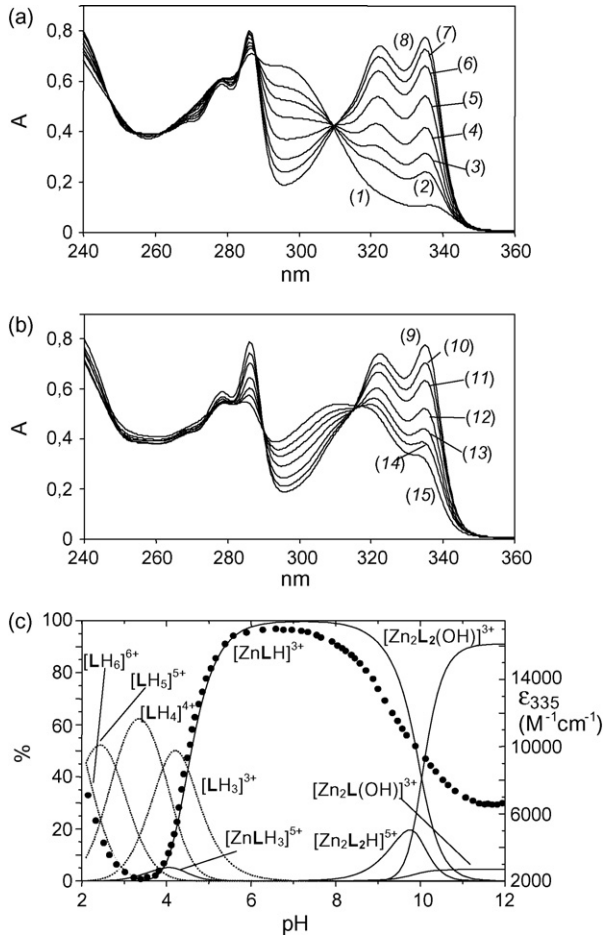

Fig. 16. UV–vis spectra recorded on aqueous solutions containing (**15**) (L) and Zn(II) in 1:1 molar ratio (a) in the pH range 3–6.5 [(1) pH 3.54, (2) 3.99, (3) 4.12, (4) 4.27, (5) 4.45, (6) 4.70, (7) 4.93, (8) 6.40] (0.1 M NMe_4Cl, T = 298.1 K) and (b) in the pH range 6–12: [(9) pH 6.40, (10) 8.57, (11) 9.00, (12) 9.57, (13) 10.12, (14) 10.53, (15) 11.52] (0.1 mol dm^{-3} NMe_4Cl, T = 298.1 K). (c) pH dependence of the absorbance at 335 nm of (**15**) in the presence of Zn(II) in 1:1 molar ratio (●, right y-axis) ([**15**] = 5.1×10^{-5} M, 0.1 M NMe_4Cl, 298.1 K), superimposed on the distribution diagram of the protonated (···) and complexed (—) species of the ligand. L = [**15**]. Reprinted with permission from Ref. [130]. Copyright 2004 American Chemical Society.

π-Stacking interactions between terpyridine groups stabilizing the dimeric complexes in solution were detected by means of spectrophotometric measurements [130]. Fig. 16 shows the UV–vis spectra recorded on an aqueous solution containing equimolar amounts of **15** and Zn(II) at different pH values. On increasing the pH, metal coordination produces important modifications in the absorption spectrum of the metal-free ligand, with the appearance of a structured red-shifted band at ca. 330 nm. These changes resemble very much those of the terpyridine Zn(II) complex shown in Fig. 8, indicating that complexation of Zn(II) by **15** takes place on the terpyridine site from acidic pH. In alkaline solutions the 330 nm band displays a marked decrease in absorbance while a new blue-

shifted band at ca. 310 nm appears (Fig. 16b). The appearance of this new band, accompanying the formation of $[Zn_2H(\mathbf{15})_2]^{5+}$ and $[Zn_2OH(\mathbf{15})_2]^{3+}$ complexes (Fig. 16c), is evidence for π-stacking interactions in these dimeric species. Analogous spectral features were obtained with Cu(II), in agreement with the presence of π-stacking interactions in all dimeric complexes formed by this metal ion in solution [130].

In contrast to Zn(II) and Cu(II), Cd(II) and Pb(II) do not form dimeric complexes in solution, although the $[\{Cd[H(\mathbf{15})]\}_2(\mu\text{-}Br)]^{5+}$ species was observed in the solid state. Cd(II) and Pb(II) form both mono- and binuclear complexes with **15**. With these metal ions, the terpyridine moiety is again the principal coordination site of the ligand as shown by spectrophotometric measurements which clearly indicate that even in the mononuclear complexes the metal ions are always coordinated to the heteroaromatic group [130].

Polyammonium macrocycles and metal complexes of macrocyclic polyamines have proved to be interesting synthetic mimics of a variety of phosphoryl transfer enzymes. The mononuclear Zn(II) complex of **15** was especially effective in the activation of ATP cleavage in the presence of an uncoordinated metal ion [77]. As noted above, this ligand forms both mono- and binuclear Zn^{2+} complexes depending on the metal-to-ligand molar ratio and the solution pH. The first Zn^{2+} ion interacting with the ligand binds to the terpyridine moiety while the second one occupies the polyamine chain. The protonated forms of the ligand as well as both mono- and binuclear complexes form stable adducts with ATP but do not cause any significant catalysis of ATP hydrolysis. The Zn(II) complexes with **15** display a markedly higher affinity for ATP than the protonated forms of the metal-free ligand, indicating the crucial role played by Zn(II) in ATP binding. ^{31}P measurements showed that the γ-phosphate group of ATP is involved in salt-bridges with the ammonium groups of the complex, while ^{1}H NMR spectra revealed that the adenine group of ATP is involved in π-stacking interactions with the terpyridine moiety of the ligand.

Only the tetraprotonated $\{Zn[H_4(\mathbf{15})]ATP\}^{2+}$ species in the presence of uncoordinated Zn^{2+} ions gives rise to fast ATP cleavage to produce ADP and phosphate. The analysis of the pH dependence of the hydrolysis rate constant (Fig. 17) clearly showed that only the tetraprotonated species is able to activate

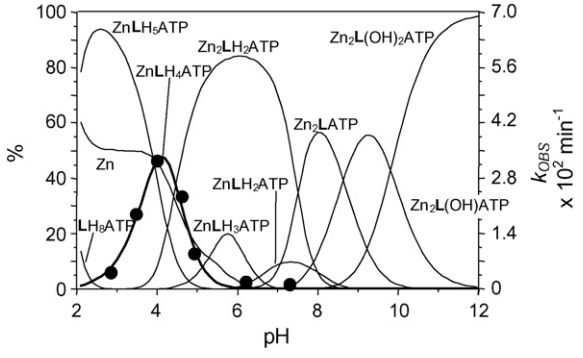

Fig. 17. Experimental pseudo-first order rate constants (●, right axis) for ATP cleavage and distribution diagram for the system Zn(II)/(**15**)/ATP in 2:1:1 molar ratio (—, left axis); 298.1 K, 0.1 M Me_4NCl. L = (**15**) [77]. Reproduced by permission of The Royal Society of Chemistry.

ATP hydrolysis, while both tri- and penta-protonated ones are completely inactive. The hydrolytic process proceeds through the formation of a phosphoramidate (PN) intermediate which is then rapidly hydrolysed to hydrogen-phosphate (Fig. 18). The pseudo first order hydrolysis rate ($k_{OBS} = 3.2 \times 10^{-2}$ min^{-1} at pH 4, 298.1 K) is among the highest observed for ATP dephosphorylation promoted by polyammonium receptors.

Nevertheless, the rate of hydrolysis increases with free Zn(II) concentration. The fact that ATP cleavage takes place only in the presence of an unbound Zn(II) ion with second order kinetics suggests that the transition state could be stabilized by this metal ion, probably through coordination of the metal to unprotonated amine groups of the macrocycle and to the γ-phosphate of ATP, leading to a higher activation of the γ-phosphorus to the nucleophilic attack. At the same time, the PN intermediate could be stabilized *via* coordination to the metal, accounting for the observed relatively high percentage of PN accumulating during the cleavage process.

The present system, therefore, represents a unique case of ATP dephosphorylation promoted by the simultaneous action of a metal complex, which is used essentially to anchor the anionic substrate, and of a second metal, which acts as cofactor, assisting the phosphoryl transfer from ATP to an amine group of the receptor. Other dizinc(II) systems containing polyazamacrocycles able to promote the hydrolysis of phosphate esters have been reported [137–146]. For these systems, however, the hydrolytic mechanism is different from that observed with **15**. In these cases both Zn(II) cations are firmly bound to the ligand and can cooperate in the binding of the substrate, while the nucleophilic agents involved in the hydrolytic processes are Zn-OH functions generated upon deprotonation of Zn(II)-coordinated water molecules.

Also in the case of the hepta-aza macrocycle **17** the connection of the polyamine chain with terpyridine in 6,6″ positions makes it possible to involve the benzylic nitrogen atoms in the coordination of metal ions. This is clearly seen in the solid state in the crystal structures of the complexes $[\{Cd[H(\mathbf{17})]\}(H_2O)_2]^{3+}$ and $[\{Pb[H(\mathbf{17})]\}Br]^{2+}$ [131]. In $[\{Cd[H(\mathbf{17})]\}(H_2O)_2]^{3+}$ the metal ion is hepta-coordinated by the three heteroaromatic nitrogen atoms, the two secondary nitrogen atoms in benzylic positions and two water molecules, defining a distorted pentagonal bipyramid with the five nitrogen atoms in the equatorial plane (maximum deviation 0.189 Å) and the water molecules in apical positions (Fig. 19a). The metal ion lies in the equatorial plane slightly shifted (0.0458 Å) towards one of the water molecules. One of the uncoordinated N-donors, not identified, is protonated. The terpyridine group is not coplanar, the largest dihedral angle (14.5°) being formed by the furthest pyridine rings.

In contrast, the Pb(II) ion in the $[\{Pb[H(\mathbf{17})]\}Br]^{2+}$ complex shows a pentagonal pyramidal coordination geometry in which the basal plane (maximum deviation 0.19 Å) is defined by the same nitrogen atoms defining the equatorial plane of the Cd(II) complex and the apical position is occupied by the bromide ion (Fig. 19b). The metal lies above the basal plane, 0.408 Å towards the bromide anion. This coordination geometry leaves a large free zone around the metal ion where a stereochemically active

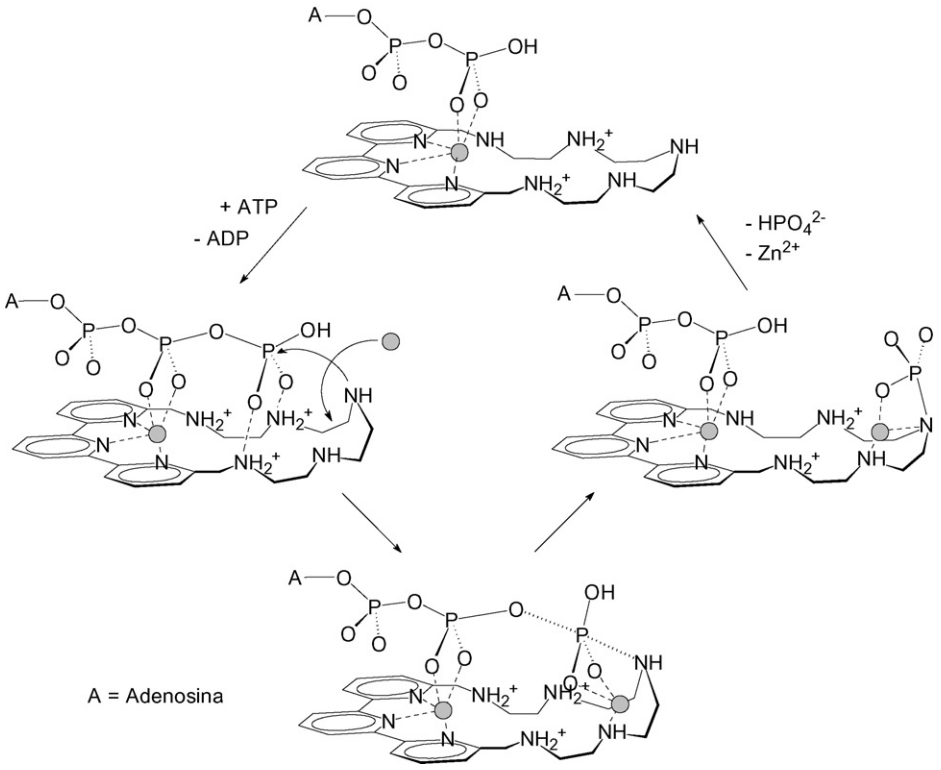

Fig. 18. Schematic representation of the ATP cleavage mechanism in the presence of $\{Zn[H_4(\mathbf{15})]ATP\}^{2+}$ and of uncoordinated Zn^{2+} ions [77]. Reproduced by permission of The Royal Society of Chemistry.

lone pair is probably localized. This is common feature shown by Pb(II) complexes which is accompanied by shortening of the coordination bonds opposite to the lone pair. In this case also one of the two nitrogen atoms not involved in the coordination is protonated. In both structures the ligand assumes a bent conformation along the axis passing through the benzylic nitrogen atoms, the dihedral angle between the two planes defined by the terpyridine unit and the four aliphatic nitrogen atoms being 38.6° and 13.98° for the Cd(II) and Pb(II) complexes, respectively.

A similar folded conformation is also assumed by the pentaprotonated $[H_5(\mathbf{17})]^{5+}$ cation found in the crystal structure of $[H_5(\mathbf{17})]Br_5{\cdot}2H_2O$. In this case folding of the molecule occurs along the axis though the benzylic methylene groups, with a dihedral angle, defined as above, of 27.8° (Fig. 20). Although the structure resolution did not allow localisation of the acidic protons, the four aliphatic amine groups form strong hydrogen bonds with two different bromide anions, strongly suggesting that they are protonated. Accordingly, the fifth acidic proton must be bound to the heteroaromatic nitrogen atoms. The terpyridine unit exhibiting the *cis*,*cis* conformation is almost coplanar, the largest dihedral angle (5.91°) being formed by the planes of the furthest pyridine rings.

The interaction of (**17**) with Cu(II), Zn(II), Cd(II) and Pb(II) in aqueous solution was studied by means of potentiometric titrations [131]. The ligand forms mononuclear $[M(\mathbf{17})]^{2+}$ complexes with all metal ions but Cu(II), which forms only pro-

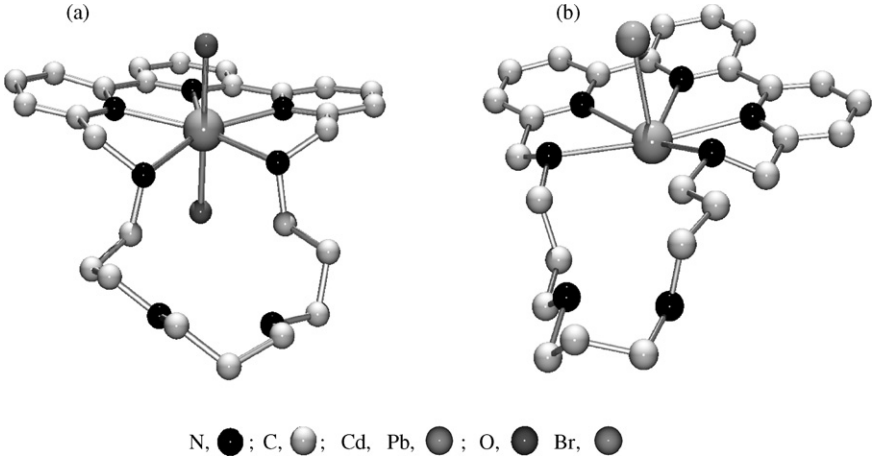

Fig. 19. Crystal structures of the $[\{Cd[H(\mathbf{17})]\}(H_2O)_2]^{3+}$ (a) and $[\{Pb[H(\mathbf{17})]\}Br]^{2+}$ (b) complex cations.

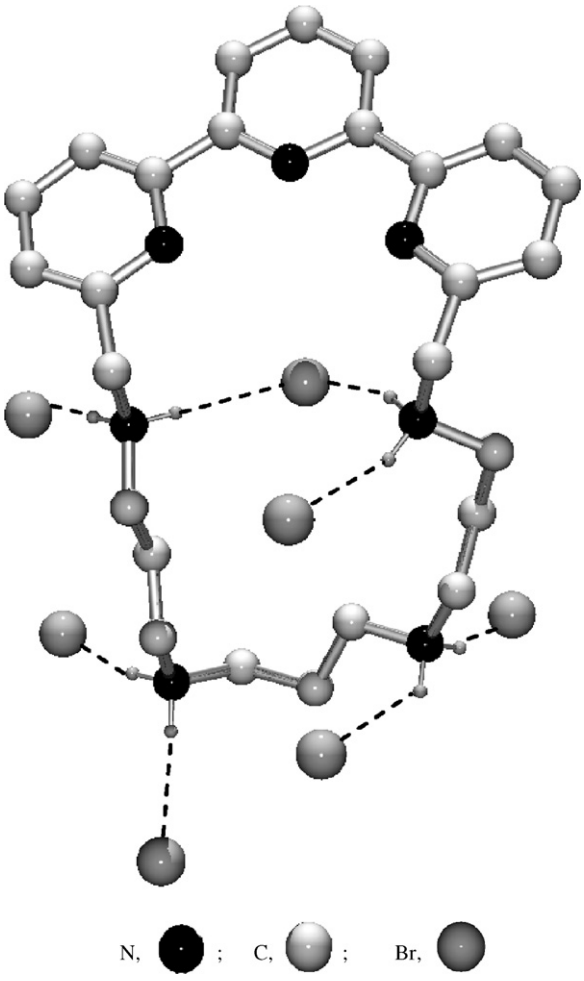

Fig. 20. Crystal structure of the $[H_5(\mathbf{17})]^{5+}$ cation.

tonated 1:1 complexes of general formula $\{M[H_n(\mathbf{17})]\}^{(n+2)+}$. These metal complexes show a marked tendency to produce protonated species, being able to bind up to three H^+ ions with the only exception of the Cd(II) complex which forms only mono- and bi-protonated species. Cu(II) gives also complexes with the unusual 2:2 stoichiometry. Moreover, **17** is able to bind two Cu(II) or Zn(II) cations, forming binuclear complexes.

Considering the 1:1 complexes, the stability of the $[M(\mathbf{17})]^{2+}$ species ($\log K = 16.1$, 11.6, 13.6 for Zn(II), Cd(II) and Pb(II), respectively) is far higher than that found for either the tetraamine ligand 1,5,9,16-tetraazatridecane [102] and terpyridine (Table 1), suggesting that both binding units are involved in metal binding, in agreement with the features of the Cd(II) and Pb(II) complex structures shown in Fig. 19. The UV spectra recorded on solutions containing the mononuclear complexes at different pH values confirm the involvement of the terpyridine group in the binding of these metal ions by the appearance of the typical structured red-shifted band at ca. 330 nm, as shown for instance in Fig. 21 for the Zn(II) complex.

In the case of Cu(II) complexes, the UV spectra displayed also characteristic features for the formation of the $[Cu_2(\mathbf{17})_2]^{4+}$ and $[Cu_2(\mathbf{17})_2OH]^{3+}$ dimeric species, as already observed for the analogous Cu(II) and Zn(II) complexes with **15** (Fig. 16),

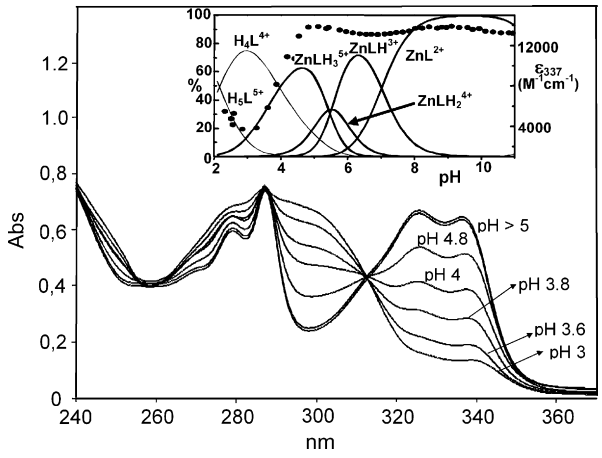

Fig. 21. UV spectra recorded on aqueous solutions containing (**17**) (L) and Zn(II) in equimolar concentrations at various pH values. Inset: pH dependence of the molar absorbance at 337 nm and species distribution diagram. $[L] = [M] = 5.1 \times 10^{-5}$ M, 0.1 M NMe_4Cl, 298.1 K [126]. Reproduced by permission of The Royal Society of Chemistry.

consisting of a decrease of the structured band at ca. 330 nm accompanied by the appearance of a new blue-shifted band at 320 nm due to π-stacking interactions of terpyridine groups within the dimeric complexes.

5. Concluding remarks

Although terpyridine was among the earliest chelating agents being explored for metal ion coordination, its use as a component of macrocyclic ligands is still a developing area prospecting numerous endeavours in the field of coordination chemistry and, in particular, in the supramolecular chemistry of coordination compounds.

Macrocyclic polyamines containing terpyridine groups are a representative class of such compounds. The main characteristic associated with the presence of terpyridine is the conformational rigidity acquired by the macrocyclic ligands, which may lead to shape-persistent molecules or to molecules containing shape-persistent regions. Terpyridine moieties are preferential binding sites for metal ions, which are forced to accept the coordination environments constructed around this terdentate group. Hence, terpyridine can be used as an efficient building block for the assembly of macrocyclic polyamine complexes with preorganized structures. In addition to the well known redox and photochemical properties of terpyridine complexes, these preorganized compounds have shown special ability in the binding and activation of particular substrates. Spontaneous CO_2 uptake from the air and conversion to carbonate, carbamination, and activation of ATP cleavage are remarkable examples described in this review.

References

[1] S.G. Morgan, F.H. Burstall, J. Chem. Soc. (1931) 20.
[2] W.R. McWhinnie, J.D. Miller, Adv. Inorg. Chem. Radiochem. 12 (1969) 135.
[3] E.C. Constable, Adv. Inorg. Chem. Radiochem. 30 (1986) 69.

[4] B. Zak, E.S. Baginsky, E. Epstein, L.M. Weiner, Clin. Chim. Acta 29 (1970) 77.
[5] B. Zak, E.S. Baginsky, E. Epstein, L.M. Weiner, Clin. Toxicol. 4 (1971) 621.
[6] J.P. Sauvage, J.P. Collin, J.C. Chambron, S. Guillerez, C. Coudret, V. Balzani, F. Barigelletti, L. De Cola, L. Flamigni, Chem. Rev. 94 (1994) 993.
[7] V. Balzani, M. Venturi, A. Credi, Molecular Devices and Machines, Wiley–VCH, Weinheim, 2003.
[8] L.F. Lindoy, I.M. Atkinson, Self-Assembly in Supramolecular Systems, Royal Society of Chemistry, Cambridge, 2000.
[9] G.R. Newkome, R. Güther, C.N. Moorefield, F. Cardullo, L. Echegoyen, E. Pérez-Cordero, H. Luftmann, Angew. Chem. Int. Ed. Engl. 34 (1995) 2023.
[10] G.R. Newkome, F. Cardullo, E.C. Constable, C.N. Moorefield, A.M.W.C. Thompson, Chem. Commun. (1993) 925.
[11] G.R. Newkome, E. He, J. Mater. Chem. 7 (1997) 1237.
[12] U.S. Schubert, C.H. Weidl, C.N. Moorefield, G.R. Baker, G.R. Newkome, Polym. Prepr. 40 (1999) 940.
[13] K. Takada, G.D. Storrier, M. Morán, H.D. Abruña, Langmuir 15 (1999) 7333.
[14] K. Mutsumi, M. Katsutoshi, H. Kenji, S. Hirofusa, Macromol. Rapid Commun. 20 (1999) 98.
[15] H.-F. Chow, I.Y.-K. Chan, P.-S. Fung, T.K.-K. Mong, M.F. Nongrum, Tetrahedron 57 (2001) 1565.
[16] D.J. Diaz, S. Bernhard, G.D. Storrier, H.D. Abruña, J. Phys. Chem. B 105 (2001) 8746.
[17] J.I. Goldsmith, K. Takada, H.D. Abruña, J. Phys. Chem. 106 (2002) 8504.
[18] G.R. Newkome, K.S. Yoo, C.N. Moorefield, Chem. Commun. (2002) 2164.
[19] K. Takada, H.D. Abruña, J. Electroanal. Chem. 567 (2004) 249.
[20] D.R. Blasini, S. Flores-Torres, D.-M. Smilgies, H.D. Abruña, Langmuir 22 (2007) 2082.
[21] M. Maskus, H.D. Abruña, Langmuir 12 (1996) 4455.
[22] U.S. Schubert, P.R. Andres, H. Hofmeier, Polym. Mater.: Sci. Eng. 85 (2001) 510.
[23] M. Heller, U.S. Schubert, Macromol. Rapid Commun. 22 (2001) 1358.
[24] M. Heller, U.S. Schubert, Macromol. Rapid Commun. 23 (2002) 411.
[25] U.S. Schubert, C. Eschbaumer, Angew. Chem. Int. Ed. 41 (2002) 2892.
[26] J.-F. Gohy, B.G.G. Lohmeijer, U.S. Schubert, Macromolecules 35 (2002) 7427.
[27] J.-F. Gohy, B.G.G. Lohmeijer, U.S. Schubert, Macromol. Rapid Commun. 23 (2002) 555.
[28] U.S. Schubert, H. Hofmeier, Macromol. Rapid Commun. 23 (2002) 561.
[29] J.-F. Gohy, B.G.G. Lohmeijer, S.K. Varshney, U.S. Schubert, Macromolecules 35 (2002) 4560.
[30] G.S. Hanan, D. Volkmer, U.S. Schubert, J.-M. Lehn, G. Baum, D. Fenske, Angew. Chem. Int. Ed. Engl. 36 (1997) 1842.
[31] A. Semenov, J.P. Spatz, M. Möller, J.-M. Lehn, B. Sell, D. Schubert, C.H. Weidl, U.S. Schubert, Angew. Chem. Int. Ed. 38 (1999) 1021.
[32] L.S. Pinheiro, M.L.A. Temperini, Surf. Sci. 464 (2000) 176.
[33] C.R. Rice, M.D. Ward, M.K. Nazeeruddin, M. Grätzel, New J. Chem. 24 (2000) 651.
[34] G. Billancia, D. Wouters, A.A. Precup, U.S. Schubert, Polym. Mater.: Sci. Eng. 85 (2001) 508.
[35] U. Ziener, J.-M. Lehn, A. Mourran, M. Möller, Chem. Eur. J. 8 (2002) 951.
[36] D.G. Kurth, M. Schütte, J. Wen, Colloid Surf. A: Physicochem. Eng. 198–200 (2002) 633.
[37] M. Grätzel, Inorg. Chem. 44 (2005) 6841.
[38] M.C. Jiménez, C.O. Dietrich-Buchecker, J.-P. Sauvage, Angew. Chem. Int. Ed. 39 (2000) 3284.
[39] J.-P. Collin, C. Dietrich-Buchecker, P. Gaviña, M.C. Jimenez-Molero, J.-P. Sauvage, Acc. Chem. Res. 34 (2001) 477.
[40] M.C. Jimenez-Molero, C.O. Dietrich-Buchecker, J.-P. Sauvage, Chem. Eur. J. 8 (2002) 1456.
[41] A. Livoreil, C.O. Dietrich-Buchecker, J.-P. Sauvage, J. Am. Chem. Soc. 116 (1994) 9399.
[42] A. Livoreil, J.-P. Sauvage, N. Armaroli, V. Balzani, L. Flamigni, B. Ventura, J. Am. Chem. Soc. 119 (1997) 12114.
[43] F. Baumann, A. Livoreil, J.-P. Sauvage, Chem. Commun. (1997) 35.
[44] D.J. Cárdenas, A. Livoreil, J.-P. Sauvage, J. Am. Chem. Soc. 118 (1996) 11980.
[45] A. Harriman, R. Ziessel, Coord. Chem. Rev. 171 (1998) 331.
[46] F. Barigelletti, L. Flamigni, V. Balzani, J.-P. Collin, J.-P. Sauvage, A. Sour, E.C. Constable, A.M.W. Cargill Thompson, J. Chem. Soc., Chem. Commun. (1993) 942.
[47] L. Flamigni, F. Barigelletti, N. Armaroli, J.-P. Collin, J.-P. Sauvage, J.A.G. Williams, Chem. Eur. J. 4 (1998) 1744.
[48] J.-P. Collin, I.M. Dixon, J.-P. Sauvage, J.A.G. Williams, F. Barigelletti, L. Flamigni, J. Am. Chem. Soc. 121 (1999) 5009.
[49] I.M. Dixon, J.-P. Collin, J.-P. Sauvage, F. Barigelletti, L. Flamigni, Angew. Chem. Int. Ed. 39 (2000) 1292.
[50] I.M. Dixon, J.-P. Collin, J.-P. Sauvage, L. Flamigni, Inorg. Chem. 40 (2001) 5507.
[51] L. Flamigni, Pure Appl. Chem. 73 (2001) 421.
[52] E. Baranoff, J.-P. Collin, L. Flamigni, J.-P. Sauvage, Chem. Soc. Rev. 33 (2004) 147.
[53] E. Baranoff, I.M. Dixon, J.-P. Collin, J.-P. Sauvage, B. Ventura, L. Flamigni, Inorg. Chem. 43 (2004) 3057.
[54] J.-P. Collin, A. Harriman, V. Heitz, F. Odobel, J.-P. Sauvage, J. Am. Chem. Soc. 116 (1994) 5679.
[55] J.-P. Collin, P. Gaviña, V. Heitz, J.-P. Sauvage, Eur. J. Inorg. Chem. (1998) 1.
[56] E.C. Constable, D. Phillips, Chem. Commun. (1997) 827.
[57] B. Hasenknopf, J.-M. Lehn, Helv. Chim. Acta 79 (1996) 1643.
[58] B. Hasenknopf, J.-M. Lehn, G. Baum, D. Fenske, Proc. Natl. Acad. Sci. U.S.A. 93 (1996) 1397.
[59] E.C. Constable, T. Kulke, M. Neuburger, M. Zehnder, Chem. Commun. (1997) 489.
[60] M. Aoyagi, K. Biradha, M. Fujita, J. Am. Chem. Soc. 121 (1999) 7457.
[61] S.-S. Sun, A.J. Lees, Inorg. Chem. 40 (2001) 3154.
[62] S.-S. Sun, A.S. Silva, I.M. Brinn, A.J. Lees, Inorg. Chem. 39 (2000) 1344.
[63] R. Ziesse, Synthesis (1999) 1839.
[64] N.W. Alcock, A.J. Clarke, W. Errington, A.M. Josceanu, P. Moore, S.C. Rawle, P. Sheldon, S.M. Smith, M.L. Turonek, Supramol. Chem. 6 (1996) 281.
[65] P.M. Gleb, U. Priimov, P.K. Maritim, P.K. Butalanyi, N.W. Alcock, J. Chem. Soc., Dalton Trans. (2000) 445.
[66] F. Loiseau, C.D. Pietro, S. Serroni, S. Campagna, A. Licciardello, A. Manfredi, G. Pozzi, S. Quici, Inorg. Chem. 40 (2001) 6901.
[67] G.R. Newkome, T.J. Cho, C.N. Moorefield, R. Cush, P.S. Russo, L.A. Godínez, M.J. Saunders, P. Mohapatra, Chem. Eur. J. 8 (2002) 2946.
[68] C.B. Smith, E.C. Constable, C.E. Housecroft, B.M. Kariuki, Chem. Commun. (2002) 2068.
[69] H.S. Chow, E.C. Constable, C.E. Housecroft, M. Neuburger, Dalton Trans. (2003) 4568.
[70] E.C. Constable, C.E. Housecroft, C.B. Smith, Inorg. Chem. Commun. 6 (2003) 1011.
[71] J.C. Loren, M. Yoshizawa, R.F. Haldimann, A. Linden, J.S. Siegel, Angew. Chem. Int. Ed. 42 (2003) 5702.
[72] P.R. Andres, U.S. Schubert, Synthesis (2004) 1229.
[73] Y. Bretonniere, M. Mazzanti, J. Pecaut, M.M. Olmstead, J. Am. Chem. Soc. 124 (2002) 9012.
[74] E.R. Schofield, J.-P. Collin, N. Gruber, J-.P. Sauvage, Chem. Commun. (2003) 188.
[75] E. Garcia-España, P. Gaviña, J. Latorre, C. Soriano, B. Verdejo, J. Am. Chem. Soc. 126 (2004) 5082.
[76] B. Verdejo, J. Aguilar, E. Garcia-España, P. Gaviña, J. Latorre, C. Soriano, J.M. Llinares, A. Doménech, Inorg. Chem. 45 (2006) 3803.
[77] C. Bazzicalupi, A. Bencini, A. Bianchi, A. Danesi, C. Giorgi, C. Lodeiro, F. Pina, S. Santarelli, B. Valtancoli, Chem. Commun. (2005) 2630.
[78] D.S.H.L. Kim, C.L. Ashendel, Q. Zhou, C.T. Chang, E.S. Lee, C. Chang, Bioorg. Med. Chem. Lett. 8 (1998) 2695.
[79] W.C. Xu, Q. Zhou, C.L. Ashendel, C.T. Chang, C.J. Chang, Bioorg. Med. Chem. Lett. 9 (1999) 2279.

[80] G. Lowe, A.S. Droz, T. Vilaivan, G.W. Weaver, J.J. Park, J.M. Pratt, L. Tweedale, L.R. Kelland, J. Med. Chem. 42 (1999) 3167.
[81] Y. Zhang, C.B. Murphy, W.E. Jones, Macromolecules 35 (2002) 630.
[82] J.B. Stimmel, M.E. Stockstill, F.C. Kull Jr., Bioconjugate Chem. 6 (1995) 219.
[83] J.B. Stimmel, F.C. Kull Jr., Nucl. Med. Biol. 25 (1998) 117.
[84] J. Costa, R. Ruloff, L. Burai, L. Helm, A.E. Merbach, J. Am. Chem. Soc. 127 (2005) 5147.
[85] R. Ruloff, G. Van Koten, A.E. Merbach, Chem. Commun. (2004) 842.
[86] H. Hofmeier, H.S. Schubert, Chem. Soc. Rev. 33 (2004) 373.
[87] U.S. Schubert, H. Hofmeier, G.R. Newkome, Modern Terpyridine Chemistry, Wiley–VCH, Weinheim, 2006.
[88] C. Grave, D. Lentz, A. Schäfer, P. Sammorì, J.P. Rabe, P. Franke, A.D. Schlünter, J. Am. Chem. Soc. 125 (2003) 6907, and references therein cited.
[89] M.G.B. Drew, M.J. Hudson, P.B. Iveson, M.L. Russel, J.-O. Liljenzin, M. Skålberg, L. Spjuth, C. Madic, J. Chem. Soc., Dalton Trans. (1998) 2973.
[90] C.A. Bessel, R.F. See, D.L. Jameson, M.R. Churchill, K.J. Takeuchi, J. Chem. Soc., Dalton Trans. (1992) 3223.
[91] K.F. Bowles, I.P. Clark, J.M. Cole, M. Gourlay, A.M.E. Griffin, M.F. Mahon, L. Ooi, A.W. Parker, P.R. Raithby, H.A. Sparkes, M. Towrie, Cryst. Eng. Commun. 7 (2005) 269.
[92] H. Elsbernd, J.K. Beattie, J. Inorg. Nucl. Chem. 34 (1972) 771.
[93] F.E. Lytle, L.M. Petrosky, L.R. Carlson, Anal. Chim. Acta 57 (1971) 239.
[94] E.C. Constable, J. Chem. Soc., Dalton Trans. (1985) 2687.
[95] P.E. Fielding, R.J.W. Le Fevre, J. Chem. Soc. (1951) 1811.
[96] K. Nakamoto, J. Phys. Chem. 64 (1960) 1420.
[97] R.P. Thummel, Y. Jahng, J. Org. Chem. 50 (1985) 2407.
[98] U. Siriwardane, N.S. Hosmane, Acta Crystallogr. C 4 (1988) 1572.
[99] C.F. Chee, K.M. Lo, S.W. Ng, Acta Crystallogr. E 59 (2003) m174.
[100] L. Prasad, F.E. Smith, Acta Crystallogr. B 38 (1982) 1815.
[101] L. Prasad, F.L. Lee, Y. Le Page, Acta Crystallogr. B 38 (1982) 259.
[102] R.M. Smith, A.E. Martell, NIST Stability Constants Database, version 4.0, National Institute of Standards and Technology, Washington, DC, 1997.
[103] A. Hergold-Brundić, Z. Popović, D. Matković-Čalogović, Acta Crystallogr. C 52 (1996) 3154.
[104] This work. ^{1}H spectra were recorded at 298 K on a Varian Unity 300 MHz instrument. Peak positions are reported relative to DMSO.
[105] A. Sarkar, S. Chakravorti, J. Lumin. 63 (1995) 143.
[106] Y. Nakayama, Y. Baba, H. Yasuda, K. Kawakita, N. Ueyama, Macromolecules 36 (2003) 7953.
[107] S. Kremer, W. Henke, D. Reinen, Inorg. Chem. 21 (1982) 3013.
[108] J.S. Judge, W.A. Baker Jr., Inorg. Chim. Acta 1 (1967) 68.
[109] E.C. Constable, J. Lewis, M.C. Liptrot, P.R. Raithby, M. Schröder, Polyhedron 2 (1983) 301.
[110] E.C. Constable, J. Lewis, M.C. Liptrot, P.R. Raithby, J. Chem. Soc., Dalton Trans. (1984) 2177.
[111] V.E. Márquez, J.R. Anacona, C. Rodriguez Barbarin, Polyhedron 20 (2001) 1885.
[112] V.E. Márquez, J.R. Anacona, D. Loroño, Polyhedron 23 (2004) 1317.
[113] L.Y. Chung, E.C. Constable, M.S. Khan, J. Lewis, P.R. Raithby, M.D. Vargas, J. Chem. Soc., Chem. Commun. (1984) 1425.
[114] E.C. Constable, F.K. Khan, J. Lewis, M.C. Liptrot, P.R. Raithby, J. Chem. Soc., Dalton Trans. (1985) 333.
[115] V.E. Márquez, J.R. Anacona, J. Coord. Chem. 49 (2000) 281.
[116] V.E. Márquez, J.R. Anacona, Transition Met. Chem. 25 (2000) 188.
[117] V.E. Márquez, J.R. Anacona, Transition Met. Chem. 29 (2004) 66.
[118] V.E. Márquez, J.R. Anacona, Polyhedron 16 (1997) 2375.
[119] E.C. Constable, J.M. Holmes, R.C.S. McQueen, J. Chem. Soc., Dalton Trans. (1987) 5.
[120] M.C. Hughes, D.J. Macero, M. Rao, Inorg. Chim. Acta 49 (1981) 241.
[121] M.C. Hughes, D.J. Macero, M. Rao, Inorg. Chim. Acta 41 (1980) 221.
[122] E.C. Constable, J.M. Holmes, Polyhedron 7 (1988) 2531.
[123] S.M. Nelson, Pure Appl. Chem. 52 (1980) 2461.
[124] P. Guerriero, P.A. Vigato, D.E. Fenton, P.C. Hellier, Acta Chem. Scand. 46 (1992) 1025.
[125] W. Radecka-Paryzek, V. Patroniak, J. Lisowski, Jerzy. Coord. Chem. Rev. 249 (2005) 2156.
[126] N.E. Borisova, M.D. Reshetova, Y.A. Ustynyuk, Chem. Rev. 107 (2007) 46.
[127] C. Galup, J.M. Couchet, C. Picard, P. Tisnès, Tetrahedron Lett. 42 (2001) 6275.
[128] C. Galup, J.M. Couchet, S. Bedel, P. Tisnès, C. Picard, J. Org. Chem. 70 (2005) 2274.
[129] J.E. Richman, T.J. Atkins, J. Am. Chem. Soc. 96 (1974) 2268.
[130] C. Bazzicalupi, A. Bencini, E. Berni, A. Bianchi, A. Danesi, C. Giorgi, B. Valtancoli, C. Lodeiro, J.C. Lima, F. Pina, M.A. Bernardo, Inorg. Chem. 43 (2004) 5134.
[131] C. Bazzicalupi, A. Bencini, A. Bianchi, L. Borsari, A. Danesi, C. Giorgi, P. Mariani, F. Pina, S. Santarelli, B. Valtancoli, Dalton Trans. (2006) 5743.
[132] D. Walther, M. Ruben, S. Rau, Coord. Chem. Rev. 182 (1999) 67.
[133] H. Ito, T. Ito, Bull. Chem. Soc. Jpn. 58 (1985) 1755.
[134] M. Aresta, D. Ballivet-Tkatchenko, D.B. Dell'Amico, M.C. Bonnet, D. Boschi, F. Calderrazzo, F. Faure, L. Labella, F. Marchetti, Chem. Commun. (2000) 1099.
[135] H. Xu, E.M. Hampe, D.M. Rudkevich, Chem. Commun. (2003) 2828.
[136] D. Belli Dell'Amico, F. Calderazzo, L. Labella, F. Marchetti, G. Pampaloni, Chem Rev. 103 (2003) 3857.
[137] H.-J. Schneider, A. Yatsimirsky, in: H. Sigel, A. Sigel (Eds.), Metal Ion in Biological Systems, vol. 40, Marcel Dekker, New York, 2003, p. 369.
[138] A. Blasko, T.C. Bruice, Acc. Chem. Res. 32 (1999) 475.
[139] E.L. Hegg, J.N. Burstyn, Coord. Chem. Rev. 173 (1998) 133.
[140] R. Krämer, Coord. Chem. Rev. 182 (1999) 243.
[141] E. Kimura, Curr. Opt. Chem. Biol. 4 (2000) 207.
[142] S. Aoki, E. Kimura, Rev. Mol. Biotechnol. 90 (2002) 129.
[143] J. Weston, Chem. Rev. 105 (6) (2005) 2151.
[144] J. Chin, Curr. Opt. Chem. Biol. 1 (4) (1997) 514.
[145] P. Scrimin, L. Baltzer, Curr. Op. Chem. Biol. 9 (6) (2005) 620.
[146] F. Mancin, P. Tecilla, New J. Chem. 6 (2007) 800.